Journal of Marine Science and Technology

Volume 21 | Issue 3 Article 12

DESIGN AND REALIZATION OF A HYBRID INTELLIGENT CONTROLLER FOR A TWIN ROTOR MIMO SYSTEM

Jih-Gau Juang
Department of Communications, Navigation and Control Engineering, National Taiwan Ocean University, Keelung, Taiwan, R.O.C, jgjuang@mail.ntou.edu.tw

Kai-Ti Tu
AmTran Technology Company, New Taipei City, Taiwan, R.O.C.

Journal of Marine Science and Technology, Vol. 21, No. 3, pp. 333-341 (2013)
DOI: 10.6119/JMST-012-1026-1

DESIGN AND REALIZATION OF A HYBRID INTELLIGENT CONTROLLER FOR A TWIN ROTOR MIMO SYSTEM

Jih-Gau Juang[1] and Kai-Ti Tu[2]

Key words: intelligent control, fuzzy switching mechanism, grey prediction, genetic algorithm, field programmable gate array.

ABSTRACT

An intelligent control scheme using a fuzzy switching mechanism, grey prediction and genetic algorithm (GA) is applied to a coupled nonlinear system, called a twin rotor multi-input multi-output system (TRMS). In real-time control, a Xilinx Spartan II SP200 FPGA (Field Programmable Gate Array) is employed to construct a hardware-in-the-loop system through writing VHDL on this FPGA. The objective is to stabilize the TRMS in significant cross-coupled conditions, and to experiment with setpoint control and trajectory tracking. The proposed scheme improves the performance of the PID controller. Control gains and parameters of the fuzzy switching mechanism are obtained by GA. Simulation results show that the proposed approach results in better performance than is achieved by conventional PID control, GA-PID control, CMAC, or fuzzy control.

I. INTRODUCTION

The TRMS control problem has been the focus of many recent studies [1, 9, 14, 19, 20]. In [1], the dynamic model of the TRMS in one-degree-of-freedom was identified by a black-box system identification technique. LQG was then applied to perform tracking control. The settling time on tracking a square wave pitch command was 6 to 7 seconds. In [20] the authors utilized a GA to search for proper PID control gains for the TRMS. This approach performed well on sine wave steady-state response; however, transient response on the main rotor took more than 30 sec. A fuzzy logic controller was proposed in [9]. Although stable tracking could be obtained, there is a large error of sine wave response. In this paper we develop an intelligent scheme to control a two-degree-of-freedom experimental propeller setup, called a twin rotor MIMO system. The proposed control scheme utilizes a fuzzy switching mechanism, grey prediction and genetic algorithm in the PID controller design.

The concept of fuzzy set theory was first proposed by Zadeh in 1965 [26], and was intended to enable handling imprecise information in the real world. Zhang [27] optimized the input/output membership functions for a nonlinear dynamic system by Extended Kalman Filter. Lu [17] used a genetic algorithm to tune the membership functions of a fuzzy controller for smart structure systems with the requirement of vibration control; independently of the expert's knowledge, this adjusted the parameters of a fuzzy controller to improve performance. In this paper, a switching mechanism is built by a fuzzy inference system to produce an appropriate forecasting step-size [23, 24]. A randomly chosen parameter set always results in poor performance. To provide a more efficient methodology for adjusting fuzzy set parameters, genetic algorithms are thus considered.

The grey system was first introduced by Deng in 1981 [4]. The following year, he proposed the grey control system, which resulted in wide and extensive study of the grey system [5]. Grey theory mainly integrates key concepts of system theory, information theory and control theory. Grey system theory has been widely utilized in system modeling, information analysis and prediction fields [7, 18, 21]. The grey prediction controller was proposed by Cheng in 1986 [3]. A large prediction step used in the grey prediction controller usually causes a worse transient response, while a small prediction step yields a faster response; therefore, the forecasting step-size in the grey prediction controller can be switched according to the error of the system during different periods of the system response. This differs from traditional prediction techniques in which predictions can still be generated by the grey model construction stage, even when facing unknown systems. Therefore, many grey prediction controller approaches have been developed in recent years [13, 16].

In this paper, the structure of a grey prediction controller is obtained by fuzzy switching mechanisms. The design process

Paper submitted 08/27/10; revised 02/03/12; accepted 10/26/12. Author for correspondence: Jih-Gau Juang (e-mail: jgjuang@mail.ntou.edu.tw).
[1] Department of Communications, Navigation and Control Engineering, National Taiwan Ocean University, Keelung, Taiwan, R.O.C.
[2] AmTran Technology Company, New Taipei City, Taiwan, R.O.C.

is more concise, and the controller is more robust than conventional controllers. The control gains of the PID controller and parameters of the fuzzy switching mechanism are obtained by GA. GA was first proposed by Holland in 1975 [8]. It is an optimization technique based on simulating the phenomena that take place in the evolution of species, and is adapted to an optimization problem. This technique implies the laws of natural selection to a population to realize individuals that are better adjusted to their environment. The population is nothing more than a set of points in the search space. Each individual of the population represents a point in that space by means of its chromosomes. The individual degree of fitness is given by the fitness function formed by system requirements. The parameters of the controller are tuned by GA, such that fitness function is formed by specific indexes such as the System Performance Index [2]. The System Performance Index is an optimization for parameters' tuning of control systems. It deals with a modification of the known integral of time multiplied by squared error criterion (ITSE). According to simulation results, the new approach improves the performances in setpoint control and trajectory tracking. In a hardware-in-the-loop system, we build a hybrid GA-PID controller in FPGA to demonstrate the proposed control scheme in the real world.

II. TRMS

The TRMS is an experimental propeller setup, as shown in Fig. 1. It is characterized by complex, highly nonlinear and inaccessible states and outputs for measurements, and hence can be considered as a challenging engineering problem [6]. The control objective is to make the beam of the TRMS move quickly and accurately to the desired attitudes, both to the pitch angle and the azimuth angle in the condition of decoupling between two axes. The TRMS is a laboratory set up for control experiments, and is driven by two DC motors. Its two propellers are perpendicular to each other, and joined by a beam pivoted on its base that can rotate freely in the horizontal and vertical planes. The joined beam can be moved by changing the input voltage to control the rotational speed of these two propellers. There is a Pendulum Counter-Weight hanging on the joined beam, which is used for balancing the angular momentum in a steady state or with a load. In certain aspects, its behavior resembles that of a helicopter. It is difficult to design a suitable controller because of the influence between the two axes and nonlinear movement. From the control perspective, it exemplifies a high order nonlinear system with significant cross coupling.

The mathematical model of a tail rotor is shown below:

$$\frac{dS_v}{dt} = l_m S_f F_v(\omega_m) - \Omega_v k_v + g((A-B)\cos\alpha_v - C\sin\alpha_v) - \frac{1}{2}\Omega_h^2 (A+B+C)\sin 2\alpha_v. \quad (1)$$

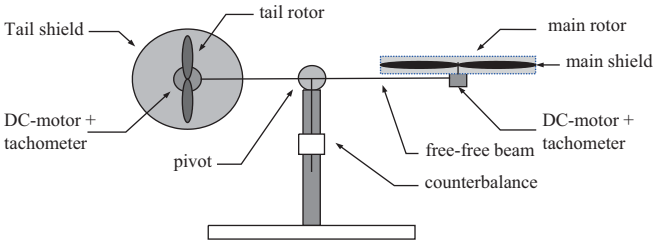

Fig. 1. The laboratory set-up TRMS.

$$\frac{d\alpha_v}{dt} = \Omega_v, \quad (2)$$

$$\Omega_v = \frac{S_v + J_{tr}\omega_t}{J_v}, \quad (3)$$

$$\frac{du_{vv}}{dt} = \frac{1}{T_{mr}}(-u_{vv} + u_v), \quad (4)$$

$$\omega_m = P_v(u_{vv}) \quad (5)$$

where

$$A = \left(\frac{m_t}{2} + m_{tr} + m_{ts}\right) l_t,\ B = \left(\frac{m_m}{2} + m_{mr} + m_{ms}\right) l_m,$$

$$C = \left(\frac{m_b}{2} l_b + m_{cb} l_{cb}\right).$$

The mathematical model of tail rotor is shown below

$$\frac{dS_h}{dt} = l_t S_f F_h(\omega_t)\cos\alpha_v - \Omega_h k_h \quad (6)$$

$$\frac{d\alpha_h}{dt} = \Omega_h, \quad (7)$$

$$\Omega_h = \frac{S_h + J_{mr}\omega_m \cos\alpha_v}{J_h} = \frac{S_h + J_{mr}\omega_m \cos\alpha_v}{D\sin^2\alpha_v + E\cos^2\alpha_v + F}, \quad (8)$$

$$\frac{du_{hh}}{dt} = \frac{1}{T_{tr}}(-u_{hh} + u_h), \quad (9)$$

$$\omega_t = P_h(u_{hh}) \quad (10)$$

where m_{mr} is the mass of the main DC motor with main rotor, m_m is the mass of the main part of the beam, m_{tr} is the mass of the tail motor with tail rotor, m_t, is the mass of the tail part of the beam, m_{cb} is the mass of the counter-weight, m_b is the mass of the counter-weight beam, m_{ms} is the mass of

the main shield, m_{ts} is the mass of the tail shield, l_b is the length of the counter-weight beam, l_{cb} is the distance between the counter-weight and the joint, J_v is the moment of inertia with respect to the horizontal axis, α_v is the vertical position (pitch position) of the TRMS beam, l_m is the arm of aerodynamic force from the main rotor, l_t is the effective arm of aerodynamic force from the tail rotor, g is the acceleration of gravity, ω_m is the rotational speed of the main rotor, $F_v(w_m)$ is the nonlinear function of aerodynamic force from the main rotor, k_v is the moment of friction force in the horizontal axis, Ω_v is the angular velocity (pitch velocity) of the TRMS beam, Ω_h is the angular velocity (azimuth velocity) of the TRMS beam, α_h is the horizontal position (azimuth velocity) of the TRMS beam, J_h is the nonlinear function of moment of inertia with respect to the vertical axis, ω_t is the rotational speed of the tail rotor, $F_h(\omega_t)$ is the nonlinear function of aerodynamic force from the tail rotor, k_h is the moment of friction force in the horizontal axis, T_{tr} is the vertical angular momentum from the tail rotor, T_{mr} is the vertical angular momentum from the main rotor, S_v is the vertical turning moment, S_h is the horizontal turning moment, S_f is the balance factor, and u_v and u_h are the DC-motor control inputs.

III. INTELLIGENT CONTROL AND SIMULATION

Grey prediction with a second order difference equation of DGM(2,1) model, a fuzzy switching grey mechanism and GA are applied to the TRMS. The structure is shown in Fig. 2, where r is the reference input, u is the control signal, y is the attitude of the TRMS, $\hat{y}$ is the prediction value, and p is the forecasting step-size for the Grey Prediction Controller. The control circuit adjusts the timing alignment between the locally generated spreading signal and the received signal. When the timing alignment is correct, the correlator output will reach its maximal value. Therefore, the code acquisition can be attained by examining the peak locations of the correlator output signal.

1. Grey Prediction Model

The proposed scheme enhances the grey prediction method of difference equations, which is a single variable second order grey model. The steps of grey prediction modeling can be summarized as follows [22]. Let $y^{(0)}$ be a non-negative original data sequence:

$$y^{(0)} = \left\{ y^{(0)}(1), y^{(0)}(2), ..., y^{(0)}(n) \right\}, n \geq 4. \quad (11)$$

Take the accumulated generating operation (AGO) on $y^{(0)}$, the AGO sequence $y^{(1)}$ can then be described by:

$$y^{(1)}(k) = \text{AGO} \circ y^{(0)} = \sum_{m=1}^{k} y^{(0)}(m), k = 1, 2, ..., n. \quad (12)$$

The DGM(2,1) model is expressed as:

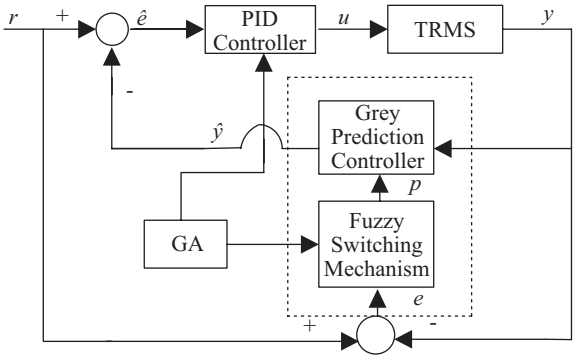

Fig. 2. The block diagram of the fuzzy switching grey prediction PID control.

$$y^{(1)}(k+2) + ay^{(1)}(k+1) + by^{(1)}(k) = 0, \quad (13)$$

where a and b are undecided coefficients of the second order difference equation. The parameters a and b can be solved by means of the least square method as follows:

$$\begin{bmatrix} a \\ b \end{bmatrix} = (Q^T Q)^{-1} Q^T Y, \quad (14)$$

where

$$Y = \begin{bmatrix} y^{(1)}(3) \\ y^{(1)}(4) \\ \vdots \\ y^{(1)}(n) \end{bmatrix}$$

$$Q = \begin{bmatrix} -y^{(1)}(2) & -y^{(1)}(1) \\ -y^{(1)}(3) & -y^{(1)}(2) \\ \vdots & \vdots \\ -y^{(1)}(n-1) & -y^{(1)}(n-2) \end{bmatrix}$$

Because the prediction model of the second order difference equation is based on the AGO data, we must take the inverse accumulated generating operator (IAGO) to get the non-negative $y^{(0)}$ data by the following relationship:

$$\hat{y}^{(0)}(k+p) = \hat{y}^{(1)}(k+p) - \hat{y}^{(1)}(k+p-1), \quad (15)$$

where p is the forecasting step-size. Based on the above description, the basic grey prediction method can be described as follows:

$$\hat{y}^{(0)} = \text{IAGO} \circ \text{DGM}(2,1) \circ \text{AGO} \circ y^{(0)}. \quad (16)$$

The response sequence of the system may be positive or negative. Therefore, we have to map the negative sequence

Table 1. Different forecasting step-size influence on the system.

Forecasting Step-size	Positive forecasting step-size	Negative forecasting step-size
Overshoot	Small	Big
Rise time	Long	Short
Steady state time	Slow	Fast
Adapt region	Close	Leave

to the relative positive sequence by some methods of data mapping. In this paper, we take the inverse mapping generating operator (IMGO), defined as follows.

Let $y^{(0)}$ be an original sequence, and $y_m{}^{(0)}$ be the MGO image sequence of $y^{(0)}$, then:

$$y_m{}^{(0)} = \mathrm{MGO} \circ y^{(0)} = \mathrm{bias} + y^{(0)}, \tag{17}$$

where the bias is a shift factor, and must be greater than $y^{(0)}$. The IMGO can then also be obtained as follows:

$$y^{(0)} = \mathrm{IMGO} \circ y_m{}^{(0)} = y_m{}^{(0)} - \mathrm{bias}. \tag{18}$$

Therefore, the modified grey prediction can be constructed by:

$$\hat{y}^{(0)} = \mathrm{IMGO} \circ \mathrm{IAGO} \circ \mathrm{DGM}(2,1) \circ \mathrm{AGO} \circ \mathrm{MGO} \circ y^{(0)}. \tag{19}$$

2. Fuzzy Switching Mechanism

In the grey prediction method, forecasting step-size is a key parameter for output prediction and is obtained by trial-and-error. The influence of different forecasting step-size on the system is shown in Table 1. To overcome the step-size problem, we have to find a proper forecasting step-size between the given positive and negative one. With proper forecasting step-size, obtained by the fuzzy switching mechanism [10, 15], the proposed controller not only can reduce the overshoot, but also entail a shorter rise time than the conventional PID controller. The switching mechanism is defined by:

$$p = \begin{cases} pys & \text{if} \quad |e| > \theta_l \\ pym & \text{if} \quad \theta_l \geq |e| > \theta_s \\ pyl & \text{if} \quad \theta_s \geq |e| \end{cases} \tag{20}$$

where p is the forecasting step-size of the system, *pys*, *pym* and *pyl* are the forecasting step-sizes for the large error, the middle error and the small error, respectively. θ_l and θ_s are the switching time of the large error and the small error, respectively.

In this fuzzy system, the absolute value of error $|e|$ has two linguistic values (PS-positive small, PB-positive big). The forecasting step-size p is the consequent variable of the fuzzy rules. The process takes two linguistic values (N-negative, PB-positive big). The membership functions of each linguistic value, and range for each fuzzy variable are described in Fig. 3, where the trapezoidal is used to describe the antecedent and consequent.

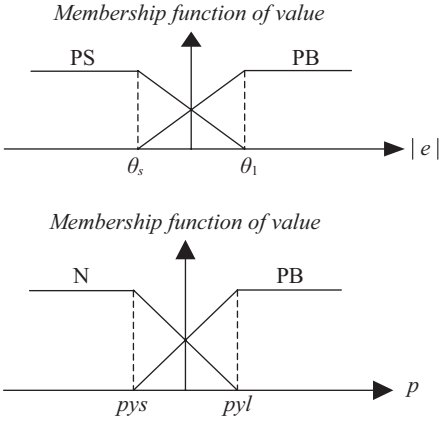

Fig. 3. Membership functions of $|e|$ and p.

The fuzzy rule base is shown as follows:

$$\begin{aligned} &\text{Rule 1: If } |e| \text{ is PS then } p \text{ is PB} \\ &\text{Rule 2: If } |e| \text{ is PB then } p \text{ is N} \end{aligned} \tag{21}$$

where (21) is employed to decide (20). The de-fuzzification process uses the discrete center of gravity method. This paper presents a fuzzy set theory with a switching grey prediction. The block diagram of the dynamic forecasting step-size is shown in Fig. 4.

3. Genetic Algorithm

In the parameter search process, a system performance index is used for fitness function in GA; this is an optimization criterion for control system parameter tuning, which is suitable for GA. It deals with a modification of the known integral of time multiplied by squared error criterion (ISTE). Population size is 10. The first step is to evaluate each fitness value of individuals (chromosomes), and to subsequently grade them by fitness function. The individuals are selected probabilistically by their fitness values. Using these selected individuals, the next population is generated through the process of a real-valued GA crossover method [10]. Mutation is applied with a very low probability: 0.025. System performance requirements are: maximum overshoot less than 10%; rising time, delay time and steady state time as short as possible. The System Performance Index is:

$$I_{PTISE} = t^n \begin{bmatrix} overshoot\ I \\ +2 \times overshoot\ II \\ +Rise\ time \\ +ssTime \end{bmatrix} + control \tag{22}$$

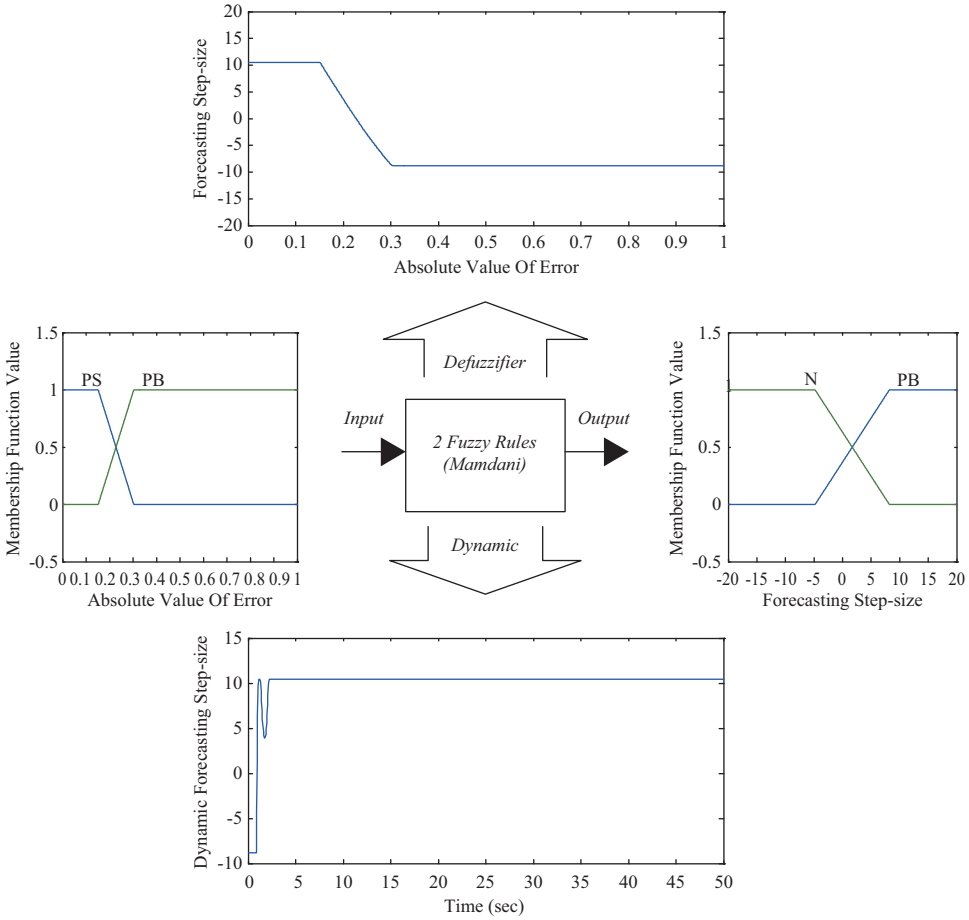

Fig. 4. Dynamic forecasting step-size change from the system error.

Rise time is the difference area between r and y, from $t = 0$ to t. The gain of y is $0.9r$. The *overshoot I & overshoot II* is the area between the overshoot or maximum peak, and r. The *control* is the absolute value of the control signal. This section is also double evaluated in the sense of more selection pressure and smooth fitness landscape. The *ssTime* is the steady state time. The fitness function in GA is:

$$Fitness\_Function = \frac{H}{I_{pitse\_h}} + \frac{V}{I_{pitse\_v}}, \qquad (23)$$

where H and V are positive constant, the values are obtained by trial-and-error. In this paper, the value 10000 is selected for H and V.

IV. SIMULATIONS

Reference input of the horizontal is 1 rad, and the initial condition is 0 rad. Reference input in the vertical is 0.2 rad, and the initial condition is -0.5 rad. Simulation time is from 0 to 50 sec, and sampling time is 0.05 sec. The target parameters in the cross-coupled system are parameters of the fuzzy switching prediction controller, pys_{hh}, pyl_{hh}, within range [-20, 20], and θ_{lhh}, θ_{shh}, within [0,1]. K_{Phv}, K_{Ihv}, K_{Dhv}, K_{Pvh}, K_{Ivh}, K_{Dvh}, K_{Pvv}, K_{Ivv}, K_{Dvv}, K_{Phh}, K_{Ihh} and K_{Dhh} of the PID controller are within range [0,1]. Simulation results are shown in Figs. 5 to 7. It can be seen that the transient response on sine wave tracking is better than [20], and that the tracking error is smaller than [9].

Different intelligent control schemes are also presented as below for comparison. The first control scheme utilized a fuzzy controller to replace the PID controller, as shown in Fig. 8 [12], where the scaling factors S_e, S_{ce}, S_{se} and S_u are adjusted by GA within the range [0, 2]. The second control scheme applied a CMAC to compensate for PID control signal, as shown in Fig. 9 [25], where u_n is the compensation for the PID control signal u_{PID}.

Comparative results of total errors from 0 to 50 seconds are shown in Table 2. Comparing the proposed controller with the conventional PID controller, total errors are reduced by 16% to 61%. Compare to control gains are tuned by binary GA [14] and real-valued GA [4], the proposed control scheme has better performance than the GA-PID control and RGA-PID control. Average performance of the proposed control system is also better than fuzzy control system [12] and CMAC control system [25], especially in vertical motion.

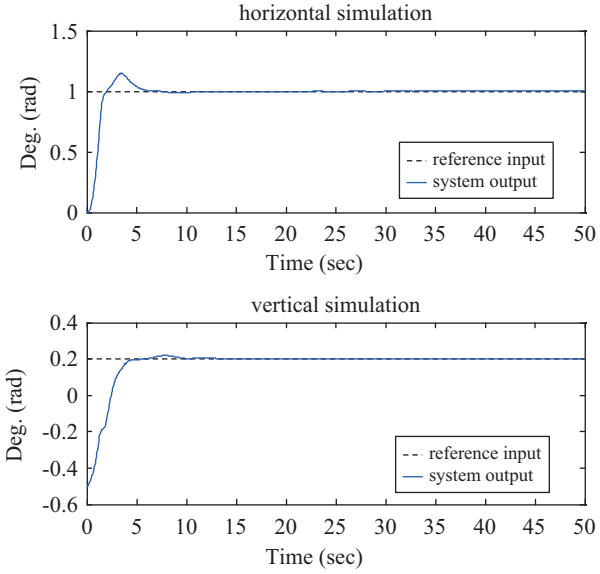

Fig. 5. Step response in cross-coupled system.

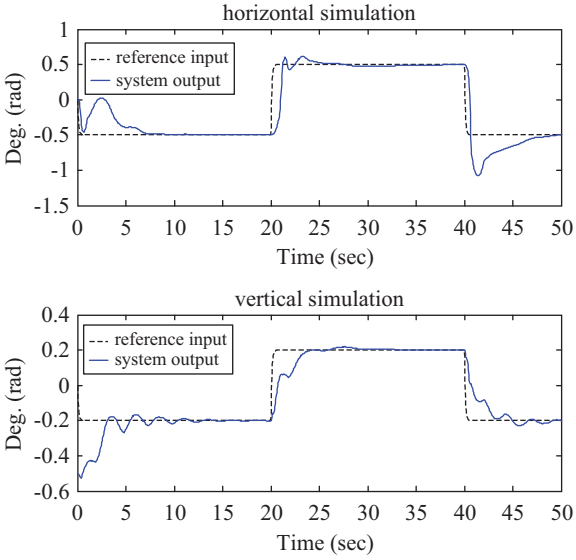

Fig. 7. Square wave response in cross-coupled system.

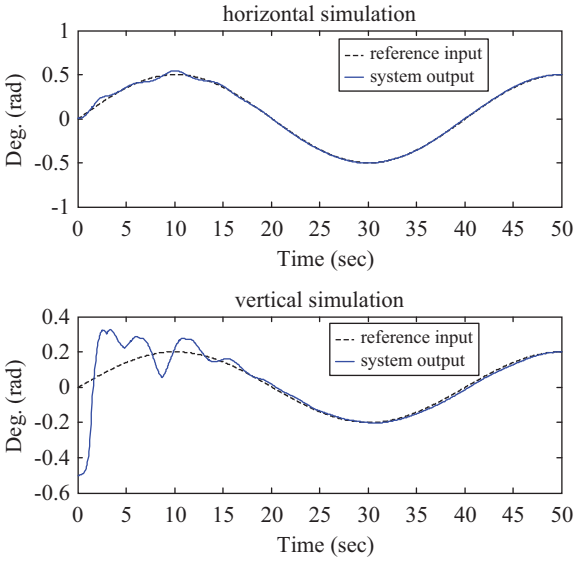

Fig. 6. Sine wave response in cross-coupled system.

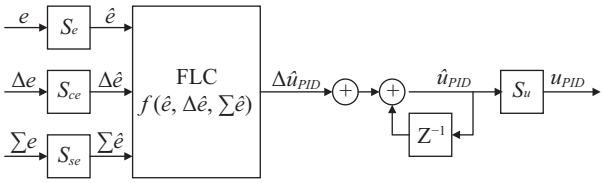

Fig. 8. Structure of fuzzy controller.

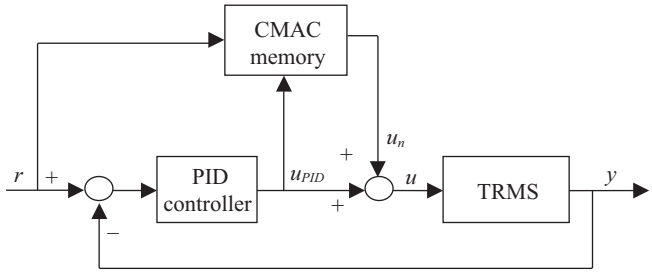

Fig. 9. Hybrid CMAC-PID control for the TRMS.

V. CONTROLLER REALIZATION

In this section, we implement the hybrid GA-PID controller in an FPGA set, the Spartan II XC2S200. The system of FPGA and TRMS is shown in Fig. 10. The control inputs to TRMS within range [0, 5] are the supply voltage of the DC motors. A change in the voltage value results in a change of the rotation speed of the propeller, which results in a change of the corresponding position of the beam. For control purpose, the position of the beam is encoded in a 16-bit code by the HCTL-2016 chip, and then combined with the FPGA which is made by Xinlinx. The command output is a 16-bit signal that will be converted to analog voltage by an AD7547 D/A converter. The design procedure is based on Foundation Series ISE 6.2 Edition. The operation frequencies of the FPGA and the HCTL-2016 are different. Two dividers are applied to divide their frequencies so that the divided results are equal.

The Spartan II XC2S200 Field-Programmable Gate Array gives high performance, abundant logic resources and a rich feature set, all at an exceptionally low price. It offers 200,000 system gates. System performance is supported up to 200 MHZ. It has a regular, flexible, programmable architecture of Configurable Logic Blocks (CLBs), surrounded by a perimeter of programmable Input/Output Blocks (IOBs). There are four Delay Locked Loops (DLLs), one at each corner of the die. Two columns of block RAM lie on opposite sides of the die, between the CLBs and the IOB columns. These

Table 2. Comparison of total error in cross-coupled system.

Reference	setpoint		sine wave		square wave	
V or H	Horizontal	Vertical	Horizontal	Vertical	Horizontal	Vertical
PID controller	81.2	40.11	23.21	65.74	150.22	112.8
GA-PID controller	50.02	32.87	14.02	72.22	125.39	99.37
RGA-PID controller	54.52	27.46	20.92	52.61	134.03	90.21
Fuzzy controller	17.28	42.54	8.26	50.55	57.03	129.2
CMAC controller	29.88	40.63	18.52	45.63	97.23	80.71
Proposed controller	28.49	27.65	8.53	43.91	101.89	38.65

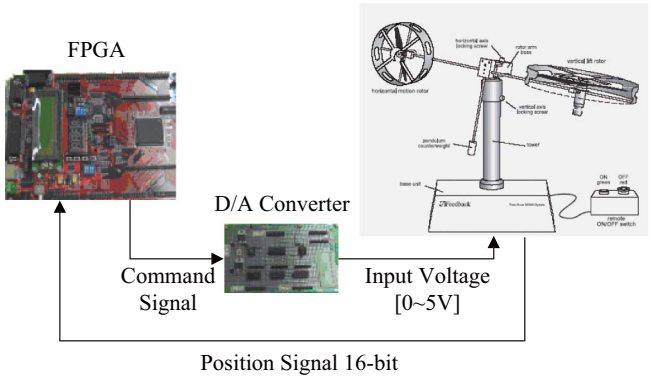

Fig. 10. System of FPGA and TRMS.

functional elements are interconnected by a powerful hierarchy of versatile routing channels. It is customized by loading configuration data into internal static memory cells. Unlimited reprogramming cycles are possible with this approach. Stored values in these cells determine logic functions and interconnections implemented in the FPGA. Configuration data can be read from an external serial PROM, or written into the FPGA in slave serial, slave parallel or Boundary Scan modes.

This FPGA is supported by Xilinx Foundation and Alliance CAE tools. The basic methodology for Spartan II design consists of three interrelated steps: design entry, implementation and verification. Industry standard tools are used for design entry and simulation (for example, Synopsis FPGA Express), while Xilinx provides proprietary architecture specific tools for implementation. It is integrated under the Xilinx Design Manager software, providing designers with a common user interface, regardless of their choice of entry and verification tools.

Implementation of GA-PID controller using FPGA is discussed below. The conventional PID controller is described as:

$$u(t) = K_P \cdot e(t) + K_I \int e(t) \cdot dt + K_D \cdot \frac{de(t)}{dt}, \qquad (24)$$

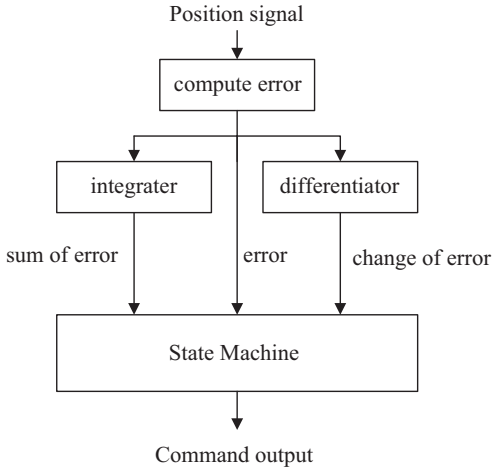

Fig. 11. Computing procedure of FPGA.

where K_p is the proportional gain, and K_I and K_D are integral and derivative time constants, respectively. Values of these control parameters are obtained by GA. The proportional term $K_P \cdot e(t)$ is implemented simply by replacing the continuous time variable with their sampled equivalence. The proportional term then becomes:

$$\pi(t_k) = K_P \cdot e(t_k), \qquad (25)$$

$$e(t_k) = e_k \text{ and } u(t_k) = u_k, \qquad (26)$$

where t_k denotes the sampling instants. When a controller is working in a wide range of operating conditions, the control variable may reach actuator limits. A pure derivative term can be written as:

$$\delta(t_k) = K_D \frac{e(t_{k+1}) - e(t_k)}{h}, \qquad (27)$$

where h is the sampling period. The integral term is:

$$\eta(t) = K_I \int_0^T e(t)dt. \qquad (28)$$

To obtain an algorithm that can be implemented in a digital device, we use the following approach to implement the GA-PID controller in FPGA:

$$\eta(t_k) - \eta(t_{k-1}) = h \cdot e(t_k) \text{ and } \eta(t_k) = \sum_{j=0}^{k} h \cdot e(t_k). \qquad (29)$$

The FPGA Computing procedure is shown in Fig. 11, where the State Machine is used for calculating command signal according to *error*, *change of error* and *sum of error*. The procedure contains some decision unit and limit switch. The whole structure of the PID controller, as shown in Fig. 12,

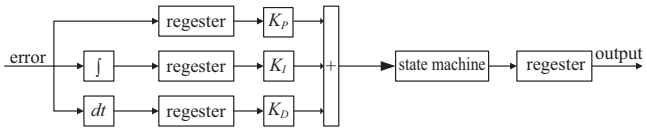

Fig. 12. Structure of PID controller.

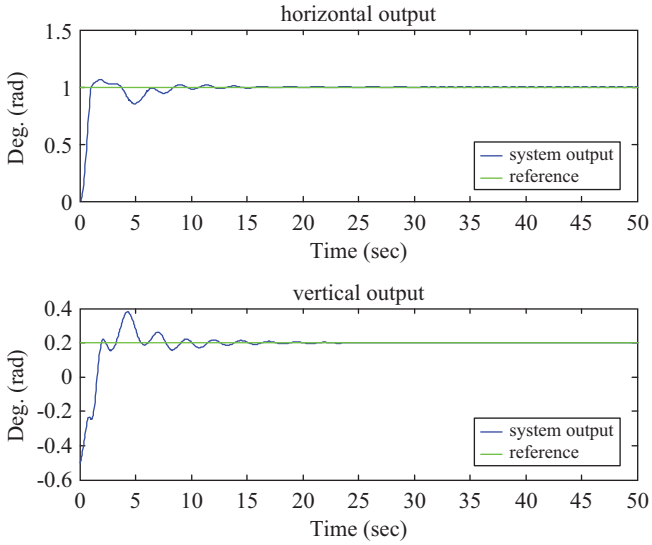

Fig. 13. System output of TRMS with proposed controller on FPGA.

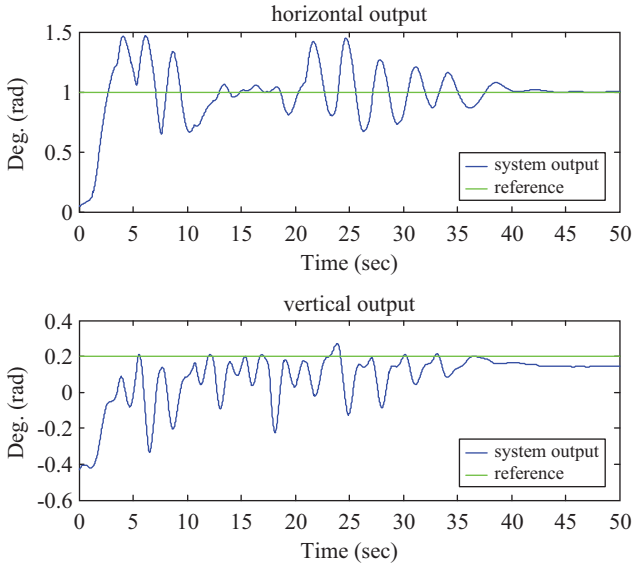

Fig. 14. System output of TRMS with conventional PID controller on FPGA.

consists of one differentiator, one integrator and 4 16-bit registers. Output is a 16-bit signal, which will be converted into analog voltage for the DC-motor.

In order to show the output performance of this implementation, VisSim real time control system is used for representing the position signal. The position signal is shown in

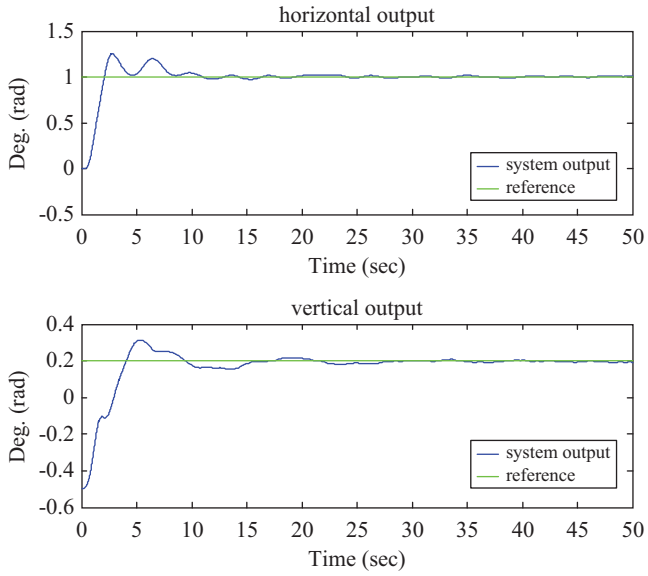

Fig. 15. System output of TRMS with fuzzy controller on FPGA.

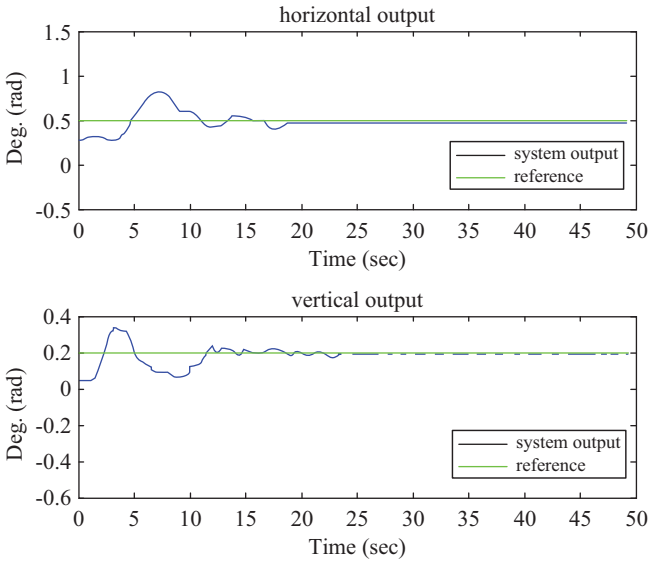

Fig. 16. System output of TRMS with CMAC controller on FPGA.

Fig. 13. The total errors in the horizontal and vertical planes are 21.78 and 68.41, respectively. Experiment results using different control schemes are shown in Figs. 14 to 16. The average performance of the proposed control scheme is better than the conventional PID control, fuzzy control, and CMAC control.

VI. CONCLUSION

This paper presents an intelligent controller design for a twin rotor MIMO system. Grey theory, fuzzy system and GA have been successfully implemented in the control scheme. The fuzzy switching mechanism with GA provides good

adaptive predictions and pre-compensations for the PID controller. This approach has successfully overcome the influence of cross-coupling between two axes. In setpoint control, it reduces maximum overshoot, rise time, steady state time and delay time. It is also suitable for simultaneously tracking a desired trajectory in the horizontal and vertical planes. In addition, the HCTL-2016 position encoding chip and Xinlinx FPGA are used for implementing the hybrid intelligent controller by coding VHDL. We analyze the position signal and convert the command signal to analog voltage in order to change propeller speed. Compared to previous works, the simulation results show that the new approach successfully reduces total error and improves system performance.

REFERENCES

1. Ahmad, S. M., Chipperfield, A. J., and Tokhi, M. O., "Dynamic modeling and optimal control of a twin rotor MIMO system," *Proceedings of the IEEE National Aerospace and Electronics Conference*, pp. 391-398 (2000).
2. Boblan, I., Koref, I. S., and Schutte, A., "A new integral criterion for parameter optimisation of dynamic systems with Evolution Strategy," *VDI BERICHTE NR*, Vol. 1526, pp. 143-150 (2000).
3. Cheng, B., "The grey control on industrial process," *Journal of Huangshi College*, Vol. 1, pp. 11-23 (1986).
4. Deng, J. L., "Control problems of unknown systems," *Proceedings of the Cilateral Meeting on Control Systems*, pp. 156-171 (1981).
5. Deng, J. L., "Control problems of grey systems," *System and Control Letters*, Vol. 1, No. 5, pp. 288-294 (1982).
6. Feedback Co, *Twin Rotor MIMO System 33-220 User Manual*, 3-000M5 (1998).
7. Han, J., Qiu, J., and Wang, Q., "On robust stability of gray discrete dynamic systems," *Advances in Systems Science and Applications*, Vol. 4, No. 3, pp. 337-340 (2004).
8. Holland, J. H., *Adaption in Natural and Artificial System*, University of Michigan Press (1975).
9. Islam, B., Ahmed, N., Bhatti, D. L., and Khan, S., "Controller design using fuzzy logic for a twin rotor MIMO system," *Proceedings of the IEEE International Multitopic Conference*, pp. 264-268 (2003).
10. Juang, J. G. and Chiou, H. K., "Turbulence encountered landing control using hybrid intelligent system," *Lecture Notes in Computer Science*, Vol. 4234, pp. 605-615 (2006).
11. Juang, J. G., Huang, M. T., and Liu, W. K., "PID control using presearched genetic algorithms for a MIMO system," *IEEE Transactions on Systems Man and Cybernetics Part C-Applications and Reviews*, Vol. 38, No. 5, pp. 716-727 (2008).
12. Juang, J. G., Lin, R. W., and Liu, W. K., "Internal model control and fuzzy control for TRMS," *Proceedings of International Automatic Control Conference*, Paper No. E102 (2007).
13. Li, C. Y. and Huang, T. L., "Optimal design of the grey prediction PID controller for power system stabilizers by evolutionary programming," *Proceedings of the IEEE International Conference on Networking, Sensing & Control*, pp. 1370-1375 (2004).
14. Liu, W. K., Fan, J. H., and Juang, J. G., "Application of genetic algorithm based on system performance index on PID controller," *Proceedings of the Ninth Conference on Artificial Intelligence and Application* (2004).
15. Liu, Z., Zhang, Y., and Wang, Y., "A type-2 fuzzy switching control system for biped robots," *IEEE Transactions on Systems, Man, and Cybernetics, Part C: Applications and Reviews*, Vol. 37, No. 6, pp. 1202-1213 (2007).
16. Lu, H. C., "Grey prediction approach for designing grey sliding mode controller," *Proceedings of the IEEE Conference on Systems, Man and Cybernetics*, pp. 403-408 (2004).
17. Lu, Q., Peng, Z., Chu, F., and Huang, J., "Design of fuzzy controller for smart structures using genetic algorithms," *Institute of Physics Publish: Smart Materials and Structures*, pp. 979-986 (2003).
18. Song, Z., "The analysis on grey element series," *Advances in Systems Science and Applications*, Vol. 5, No. 2, pp. 234-238 (2005).
19. Su, J. P., Liang, C. Y., and Chen, H. M., "Robust control of a class of nonlinear systems and its application to a twin rotor MIMO system," *Proceedings of the IEEE International Conference on Industrial Technology*, pp. 1272-1277 (2002).
20. Wang, W. Y., Lee, T. T., and Huang, H. C., "Evolutionary design of PID controller for twin rotor muti-input multi-output system," *Proceedings of World Congress on Intelligent Control and Automation*, pp. 913-917 (2002).
21. Wang, Y., Bao, Y., and Zhang, J., "A safety-focusing grey evaluation model on nuclear power plant equipment suppliers," *Advances in Systems Science and Applications*, Vol. 5, No. 2, pp. 239-244 (2005).
22. Wen, K. L., Chen, F. H., and Huang, M. L., "Existence of grey model GM (2,1)," *The Journal of Grey System*, Vol. 10, No. 3, pp. 209-214 (1998).
23. Wong, C. C. and Chen, C. C., "Switching grey prediction PID controller design," *The Journal of Grey System*, Vol. 9, No. 4, pp. 323-334 (1997).
24. Wong, C. C., Lin, B .C., and Cheng, C. T., "Fuzzy tracking method with switching grey prediction for mobile robot," *Proceedings of the IEEE International Conference on Fuzzy Systems*, pp. 103-106 (2001).
25. Yu, Z. R. and Juang, J. G., "Application of hybrid CMAC-PID control to TRMS and FPGA implementation," *Proceedings of National Symposium on System Science and Engineering*, ID-525 (2010).
26. Zadeh, L. A., "Fuzzy sets," *Information and Control*, Vol. 8, pp. 338-352 (1965).
27. Zhang, N. and Wunsch, D. C., "An extended Kalman filter (EKL) approach on fuzzy system optimization problem," *Proceedings of the IEEE International Conference on Fuzzy Systems*, pp. 1465-1470 (2003).